agriculture

MDPI

Article

Design and Performance Evaluation of a Multi-Point Extrusion Walnut Cracking Device

Hong Zhang [1,2], Hualong Liu [1,2], Yong Zeng [1,2,*], Yurong Tang [1,2], Zhaoguo Zhang [3] and Ji Che [4]

[1] College of Mechanical and Electronic Engineering, Tarim University, Alar 843300, China
[2] Agricultural Engineering Key Laboratory, Ministry of Higher Education of Xinjiang Uygur Autonomous Region, Tarim University, Alar 843300, China
[3] Faculty of Modern Agricultural Engineering, Kunming University of Science and Technology, Kunming 650000, China
[4] Xinjiang Jiangning Light Industry Mechanical Engineering Technology Co., Ltd., Urumqi 830011, China
* Correspondence: 120190040@taru.edu.cn; Tel.: +86-155-0457-7650

Abstract: The practical problems of existing methods of walnut cracking under compression loading, including incomplete walnut-shell crushing, broken walnut kernels, and so on, are widespread in walnut processing and are constraints that hinder mechanized walnut processing. Therefore, attempts have been made to design and optimize a multi-point extrusion walnut cracking device. For this, walnuts were fed manually into a cracking unit through the hopper. The tangential force of the grading roller graded the walnuts and dropped them into the gap between the rotating cracking roller and extrusion plate, causing them to crack. The developed machine was tested and the parameters were optimized using a central composite design (CCD). The objective functions involving the cracking angle (CA: 0.17, 0.27, 0.52, 0.76, 0.86°) and roller speed (RS: 63, 75, 105, 135, 147 r/min) were calculated. The shell cracking rate (*SCR*), whole kernel rate (*WKR*), and specific energy consumption (Es) regression models were established using the quadratic regression orthogonal combination test and the parameters were optimized using MATLAB software. The results showed that the most significant factors for the RS were the linear terms of the *SCR* and *WKR*, whereas for the CA the most significant factor was the linear term of the Es. The interaction term of the two factors had a significant effect on the three indicators. The optimal parameter combination was determined to be 0.47° for the CA and 108 r/min for the RS. On this basis, the adaptability test showed that the cracking device had a better cracking effect on walnuts with a gap between the walnut shell and kernel greater than 1.6 mm and a shell thickness less than 1.2 mm. The results have practical significance for the design of walnut cracking devices.

Keywords: walnut; multi-point extrusion; central composite design (CCD); parameter optimization

Citation: Zhang, H.; Liu, H.; Zeng, Y.; Tang, Y.; Zhang, Z.; Che, J. Design and Performance Evaluation of a Multi-Point Extrusion Walnut Cracking Device. *Agriculture* **2022**, *12*, 1494. https://doi.org/10.3390/agriculture12091494

Academic Editor: Bengang Wu

Received: 11 August 2022
Accepted: 13 September 2022
Published: 18 September 2022

1. Introduction

The Walnut (*Juglans regia* L.) is one of the oldest cultivated fruit species in the world [1]. The kernels have excellent nutritional and therapeutic value due to their high content of unsaturated fatty acids [2] and abundant amino acids and minerals [3,4]. In post-harvest and processing, compared to other operations (e.g., cleaning, drying, storing, etc.), walnut-shell cracking to extract the kernel from the internal nut is not only the most important operation but also the fundamental goal, which can be attributed to the fact that the usable part of tree nuts is not the walnut itself but the kernel, especially the whole kernel because consumers prefer whole kernels [5]. However, during the process of walnut cracking, unexpected phenomena (e.g., incomplete nutshell cracking and broken nut kernels) occur with existing cracking devices, which are the key factors that affect the quality of the final kernel and limit the development of the initial processing [6]. The cracking performance is strongly related to the intrinsic properties of the walnut (e.g., shell thickness and moisture content), cracking device configurations (e.g., roll and hammer), and operational conditions (e.g., shaft rotation speed). Hence, several researchers have proposed a series of effective methods to improve cracking performance in terms of the three aspects mentioned above [7–9], particularly the latter two factors.

Li [10] studied the effects of the gap between the two rotating cracking rollers and roller speed on walnut cracking. It was found that increasing the rotational speed and decreasing the pitch increased the fracture force, thereby resulting in an increase in the specific deformation of the walnut shell [11]. Shi et al. [12] evaluated a cam rocker bidirectional extrusion walnut cracking device using squeeze clearance, camshaft speed, and walnut circumference as the test factors. Bernik et al. [5] investigated the cracking quality of three types of walnuts at different speeds under a modified centrifugal cracking machine. By analyzing the above-mentioned research, it was found that the contact type between the walnut and the cracking device was mostly a single point or line load. However, it was also found that the contact types mentioned above would result in uneven forces on the shell, poor crack extension, and easy damage to the inner kernel [13]. Additionally, studies have also suggested that different contact types have a significant effect on walnut cracking. For example, Zhang et al. [14] reported that spherical compression was the best process for walnut cracking. In addition, Shen [15] discovered that adding spikes to the surface of the V-indenter for shell cracking was substantially more successful. According to the above analyses, increasing the stress concentration areas contributes to the generation and expansion of cracks while reducing the inner shell force and deformation value of walnut kernels, thus further minimizing mechanical damage to the kernels.

Unfortunately, there are few practical applications for walnut cracking devices based on multiple load contact. For instance, Cao et al. [13] observed superior walnut-cracking outcomes using a hammer head with seven grooves. Furthermore, He et al. [16] improved cracking device performance by adding rectangular or trapezoidal grooves to the surfaces of the cracking rollers. Nonetheless, the quality of cracking still needs to be improved. Therefore, by integrating the results of previous research, a multi-point extrusion walnut cracking device was designed and its operating parameters were optimized using the RSM in this work. The influence of each factor on the evaluation index and the interaction between the factors were analyzed, respectively. The best combinations of parameters were determined using the regression analysis method with the help of MATLAB software, which was used to verify the practical suitability of several walnut varieties.

2. Materials and Methods

2.1. Materials

'Wen 185', which is the typical walnut cultivar in the local market, was selected and used as the experimental sample. In the harvest season of 2021, fresh-harvested walnuts (*Juglans regia* L.) were collected from the Wensu Walnut Experimental Station (latitude: 41°27′67″ N, longitude: 80°24′17″ E, and at a 1056 m altitude), Xinjiang, China. A moderate walnut moisture content is known to improve the quality of cracking [17]. Thus, according to our previous study [18], walnut shells with a moisture content range of 7–9% and kernels with a moisture content range of 10–13% were used in the walnut cracking experiments.

2.2. Principles of a Walnut Cracking Device

A walnut cracking machine, including the frame, control panel, speed-regulating motor, feed hopper, grading cylinder, deflector, and cracking device (Figure 1a), was designed and manufactured. A control panel was used to adjust the speed of the grading cylinder and rotating cracking roller to meet the requirements of different working conditions. After feeding, the walnuts were rolled with the cylinder and were moved forward by the driving of the helical steel ribs. Different walnut sizes fell off the corresponding spaces of the cylinder and the walnuts were graded according to their size. Walnuts fell through the guide chute into the cracking device, which was composed of a rotating cracking roller and extrusion plate with 'V' grooves. The wedge-shaped space formed by the extrusion plate and rotating cracking roller was the part where the walnuts were cracked by the squeezing-type device. The space could be adjusted by the retainer bolt and the position-limit mechanism as a means of adapting to the different walnut dimensions. The shells were cracked by the squeezing, rolling, and grinding of the extrusion plate and rotating cracking roller and then ejected. In order to ensure the appropriate extrusion shearing forces on the walnut, several spikes were added to the surface of the rotating cracking roller and extrusion plate (Figure 1b) to increase the stress concentration areas. Thus, this designed cracking machine was able to simultaneously carry out walnut grading and cracking. The main technical parameters of the walnut cracking device are listed in Table 1.

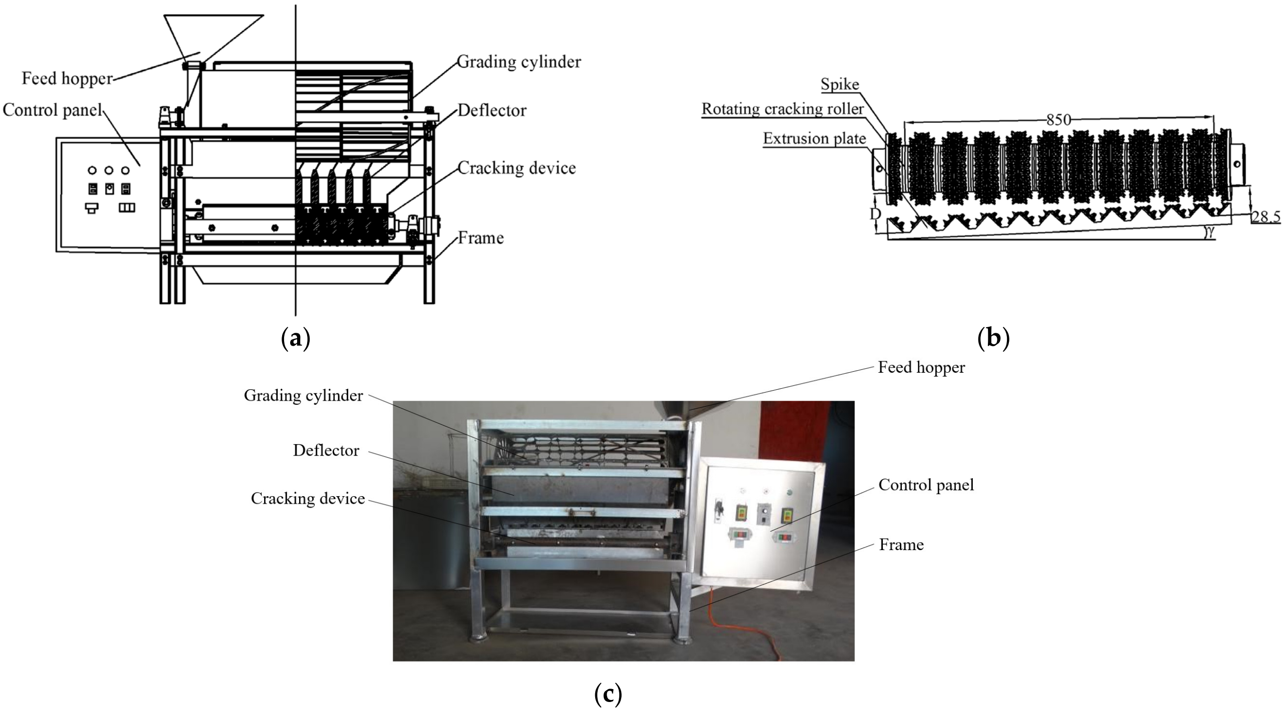

Figure 1. Overall structural schematic diagram of the walnut cracking device: (**a**) final assembly drawing, (**b**) the gap between rotating cracking roller and extrusion plate, (**c**) structural schematic photo of the prototype.

Table 1. Parameters of the cracking device.

Parameters	Size
Length × width × height/(mm × mm × mm)	1200 × 800 × 1200
Overall weight/kg	165
Inlet size/(mm × mm)	90 × 45
Productivity/(kg/h)	1080
Power of cracker/kw	0.75
Grading accuracy/(%)	≥96
Cracking angle/(°)	0–1
Roller speed/(r/min)	0–210

2.3. Design of Grading Cylinder

The length (L), width (W), and thickness (T) [17] of 200 randomly selected walnuts were measured (Figure 2) using a DELI DL91150 digital caliper (DELI Group Co., Ltd., Ningbo, China) with an accuracy of 0.01 mm. To classify the walnuts more accurately, the equivalent diameter of walnut samples was calculated based on Equation (1) mentioned in Zeng et al. [19] and the statistical results are shown in Figure 3. The measurements showed that the measured diameters conformed to a normal distribution and were mainly in the range of 32–42 mm ($p < 0.05$). The proportion of walnuts sized 32–37 mm was 34.74%, sized

37–39 mm was 35.26%, and sized 39–42 mm was 30%, respectively. Thus, based on these size distributions, the rotary fence cylinder of the walnut grader with three stages was designed as shown in Figure 4, namely, the gaps between the fences were 37 mm, 39 mm, and 42 mm, respectively.

$$D_P = \left[\frac{(W+T)^2}{4}L\right]^{\left(\frac{1}{3}\right)} \tag{1}$$

where D_P is the walnut equivalent diameter (mm); L is the length (mm); W is the width (mm); T is the thickness (mm).

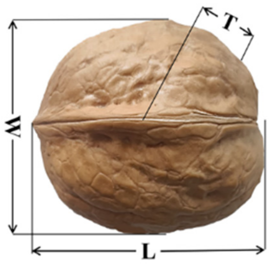

Figure 2. Characteristic parameter analysis of walnuts.

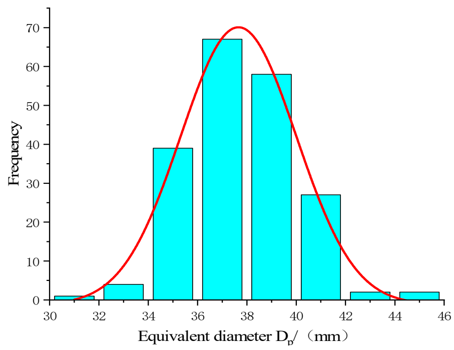

Figure 3. Equivalent diameter distribution of walnuts.

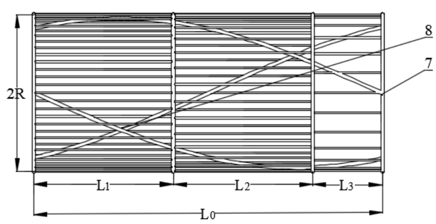

Figure 4. Schematic diagram of grading cylinder.

The grading cylinder diameter was calculated, as per Jeffrey et al. [20] where the grading cylinder speed is equal to 50% of the critical speed.

$$R = \frac{1}{2}\left(\frac{0.19Q_m}{F_i K_v d_b g^{0.5} \tan\alpha}\right)^{0.4} \tag{2}$$

of which,

$$K_v = \begin{cases} 1.35 & (\alpha = 3^\circ) \\ 1.85 & (\alpha = 5^\circ) \end{cases} \tag{3}$$

where Q_m is the feeding capacity (kg/h); α is the angle of inclination of the grading cylinder (°); K_v is the velocity correction factor; d_b is the material bulk density (kg/m^3); g is the acceleration due to gravity (m/s^2); F_i is the filling degree, taken as 0.25–0.33. Substituting

Q_m = 1080 kg/h, F_i = 0.25, α = 5°, K_v = 1.85, d_b = 470 kg/m^3 [13], and g = 9.8 m/s^2 into Equation (2) gives a grading roller radius of R = 0.16 m.

The length of the grading cylinder is related to the tumbling time of the walnuts in the grading cylinder. As the length increases, the grading time also increases, and the grading accuracy increases. However, the length should not be too long. After the length exceeds a certain value, it does not significantly increase the grading efficiency but increases the cost of the grading cylinder. Thus, the length of the grading cylinder is generally taken to be 2–6 times its diameter [21].

The length of the grading cylinder was calculated as follows where the classifying cylinder speed is equal to 50% of the critical speed.

$$L_0 = 15\sqrt{2}K_v(2R)^{0.5}g^{0.5}\pi^{-1}t_i \tan\alpha \tag{4}$$

where t_i is the residence time (min); L_0 is the grading cylinder length (m).

Substituting K_v = 1.85, R = 0.18 m, t_i = 0.5 min, and α = 5° into Equation (4), we obtain L_0 = 0.97 m, taking L_0 = 1 m. To ensure the accuracy and efficiency of grading, the grading roller is divided into 3 grades according to the proportions of the different sizes of walnuts (L_1 = L_2 = 0.35 m, L_3 = 0.3 m), as shown in Figure 4.

2.4. Design of Rotating Cracking Roller, Extrusion Plate, and Cracking Angle

For extrusion-style devices, the gap between the rotating cracking roller and extrusion plate and the speed of the rotating cracking roller are both principal factors. The gap significantly influences the deformation degree of the walnut shells, whereas the speed has an important impact on the efficiency of the walnut cracking [22]. The conditions under which walnuts can enter the gap between the rotating cracking roller and extrusion plate are as follows (Figure 5).

$$mg + \mu F_N + \mu F_R \cos\varepsilon > F_R \sin\varepsilon \tag{5}$$

Because of $\sum F_x$ = 0, bring F_N = F_R cos ε + μ F_R sin ε into Equation (5) then,

$$mg + \mu F_R \cos\varepsilon + \mu^2 F_R \sin\varepsilon + \mu F_R \cos\varepsilon > F_R \sin\varepsilon \tag{6}$$

Bring μ = tan β into Equation (6), then,

$$\varepsilon < \sin^{-1}\left(\frac{mg\cos^2\beta}{F_R}\right) + 2\beta \tag{7}$$

where F_R is the positive pressure of the rotating cracking roller on the walnut (N); F_N is the positive pressure of the extrusion plate on the walnut (N); ε is the angle between the positive pressure F_R and the horizontal line (°); β is the friction angle between the rotating cracking roller and extrusion plate and the walnut (°); μ is the friction coefficient between the rotating cracking roller, extrusion plate, and walnut, μ = tan β.

A cross-sectional view of the walnut along the thickness direction is shown in Figure 6. The walnut is squeezed into the gap in the direction of its thickness under the following conditions:

$$t < e \leqslant t + 2h \tag{8}$$

Or,

$$t < e \leqslant T - d \tag{9}$$

where e is the gap between the rotating cracking roller and extrusion plate (mm); h is the walnut shell thickness (mm); t is the wide diameter of the kernel (mm); d is the space between the kernel and the inner wall of the shell (mm), i.e., the gap between the walnut shell and kernel.

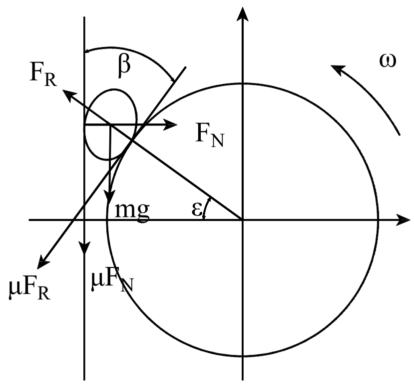

Figure 5. Forces of walnut in extrusion cracking device.

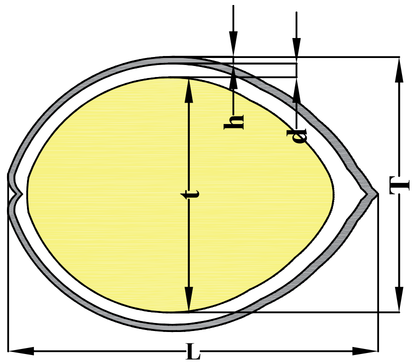

Figure 6. Transverse sectional view of a walnut.

The gap between the rotating cracking roller and extrusion plate was the largest when $e = t + 2h$ or $e = T - d$. At this point, the shell was subjected to a squeezing pressure, whereas the squeezing pressure on the kernels was zero. This is the ideal state for walnut cracking so the kernels are not damaged. When $t < e \leq t + 2h$ or $t < e \leq T - d$ was met, the external shell was just crushed but the internal kernel was not broken. The gap (d) between the walnut shell and kernel was generally 1.85 mm and the shell thickness (h) was 0.86 mm for the 'Wen 185' [23]. Thus, the minimum gap (e) was designed to be 28.5 mm.

The small end of the gap between the rotating cracking roller and the extrusion plate (right end in Figure 1b) was used as an example for the analysis. The walnut shape is assumed to be ellipsoidal [20], and then we have

$$\cos\varepsilon = \frac{r + e}{r + W} \tag{10}$$

Simplifying Equation (10), the radius of the rotating cracking roller is given by

$$r = \frac{e - W\cos\varepsilon}{\cos\varepsilon - 1} \tag{11}$$

In summary, the radius the of rotating cracking roller was 75 mm. If the gap (e) became smaller and the rotating cracking roller diameter remained the same so that $\varepsilon \geq \sin^{-1}((mg\cos^2\beta)/F_R) + 2\beta$, the cracking device did not work properly. In this paper, the gap (e) was replaced by the angle between the rotating cracking roller and extrusion plate, which was treated as a studied factor, as shown in Figure 1b. Note that the angle could be adjusted by the bolt (GB/T 5782M12 × 80) and a DELI DL305300 full-circle protractor (DELI Group Co., Ltd., Ningbo, China) with an accuracy of 0.3°. According to the above analysis and Equation (12), the cracking angle (γ) was selected in the range of 0 to 1°.

$$\tan\gamma = \frac{(D - 28.5)}{850} \tag{12}$$

where D is the big end of the gap between the rotating cracking roller and extrusion plate (mm); γ is the angle of the rotating cracking roller and extrusion plate (°).

2.5. Cracking Quality Index Measurement Method

2.5.1. Shell-Cracking Rate

To evaluate the performance of walnut cracking under different working parameters, the shell cracking rate was treated as the evaluation index, as per Zhang et al. [14], as shown in Equation (13):

$$SCR = \left(1 - \frac{M_1}{M_0}\right) \times 100\% \tag{13}$$

where SCR is expressed as the shell-cracking rate achieved in one pass through the machine (%); M_0 is the total weight of the walnuts (kg); M_1 is the mass of unbroken walnuts (kg). As shown in Figure 7, a degree of walnut breakage greater than one-half the size of a walnut was identified as a broken walnut. Among them, one-quarter walnuts and one-half walnuts were identified as shell-wrapped kernels.

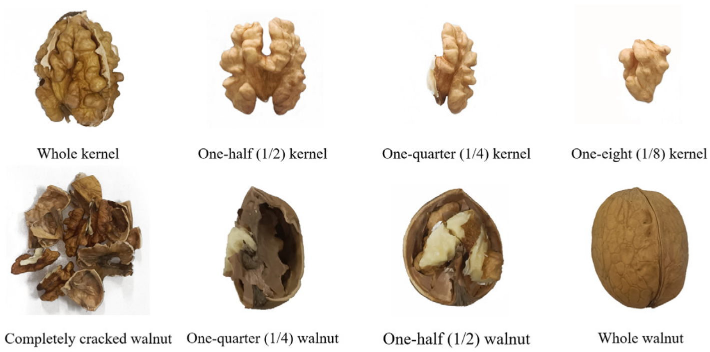

Figure 7. The different particle sizes of cracked walnuts and walnut kernels.

2.5.2. Whole Kernel Rate

Following walnut cracking, each kernel was visually evaluated to determine the state of the kernel. Each kernel was visually classified into four types, as shown in Figure 7. Kernels with greater than a 1/4 volume were defined as a "complete kernel" [17]. The WKR can be calculated by using:

$$WKR = \frac{M_3}{M_2} \times 100\% \tag{14}$$

where M_2 is the total mass of kernels obtained after cracking (kg); M_3 is the mass of kernels identified as greater than 1/4 kernels after cracking (kg).

2.5.3. Specific Energy Consumption

The energy consumption of cracking was measured using a power meter (DL333502, Deli Group Co., Ltd., Ningbo, China). The power meter was connected to a power source and the cracking device was connected to the power meter. The energy required for operating the machine without load was first recorded and then subtracted from the energy data collected when the machine was running under load. The real-time power and cracking duration were recorded during the running periods. The Es was calculated using the method of Meng et al. [24]:

$$Es = \frac{\int_0^t (P_t - P_0)dt}{M} \tag{15}$$

where P_t is the real-time power during the cracking process (W); P_0 is the operating power without walnuts in the hopper (W); t is the cracking duration (s).

2.6. Experimental Design and Statistical Analysis

Each experiment with 5 kg of 'Wen-185' walnuts (electronic balance, precision 0.01 g) was conducted and then repeated three times. The results were averaged and the data were recorded as shown in Table 2. A central composite design (CCD) of two variables (CA, RS) with five levels was adopted using the Design Expert software program (V8.0.6, Stat-Ease Co., Minneapolis, MN, USA). The range of values for the single factors was selected according to the preliminary experiments (not shown). The variables and their levels are given in Table 2. A multiple regression analysis was carried out to obtain an empirical model for each response variable, namely, the *SCR*, *WKR*, and Es. The second-order polynomial of the following forms was fitted to the data of the response.

$$Y = \beta_0 + \sum_{i=1}^{2} \beta_i X_i + \sum_{i=1}^{2} \beta_{ii} X_i^2 + \beta_{ij} X_i X_j \tag{16}$$

where Y represents the dependent responses; β_i, β_{ii}, and β_{ij} represent the regression coefficients of the process variables; X_i and X_j are coded as independent variables. Analysis of variance (ANOVA) was used to test the adequacy of the acquired model. The validity of the model was confirmed by the equation analysis, lack of fit ($p = 0.05$) tests, and R^2 (the ratio of the explained variation to the total variation) analysis. The variable level combinations and responses of the experiments are shown in Table 2. A numerical optimization module in the software was used to obtain the optimal operating parameters.

Table 2. Design and results of the experiments.

Test NO.	X_1 (°)	X_2 (r/min)	*SCR*/(%)	*WKR*/(%)	*Es*/(kJ/kg)
1	0.27 (−1)	75 (−1)	93.66	81.62	2.26
2	0.76 (1)	75 (−1)	93.52	82.36	1.92
3	0.27 (−1)	135 (1)	99.54	88.23	3.41
4	0.76 (1)	135 (1)	94.82	81.36	1.84
5	0.17 (−1.414)	105 (0)	99.42	87.98	2.62
6	0.86 (1.414)	105 (0)	95.14	83.64	2.26
7	0.52 (0)	63 (−1.414)	92.66	81.46	1.89
8	0.52 (0)	147 (1.414)	93.81	87.28	2.84
9	0.52 (0)	105 (0)	97.62	91.02	1.64
10	0.52 (0)	105 (0)	98.65	92.15	1.72
11	0.52 (0)	105 (0)	97.85	93.89	1.35
12	0.52 (0)	105 (0)	97.35	91.78	1.92
13	0.52 (0)	105 (0)	98.84	94.26	1.82

Note: X_1 cracking angle, X_2 roller speed, *SCR* shell-cracking rate, *WKR* whole kernel rate, *Es* specific energy consumption.

The degree of influence of every factor in the model can be reflected by the magnitude of the contribution ratio K, which is proportional to the magnitude of the influence [25]. Its calculation is shown in Equations (17) and (18):

$$\delta = \begin{cases} 0 & F \le 1 \\ 1 - \frac{1}{F} & F > 1 \end{cases} \tag{17}$$

$$K_j = \delta_j + \frac{1}{2} \sum_{\substack{i=1 \\ i \neq j}}^{m} \delta_{ij} + \delta_{jj} \quad j = 1, 2, \cdots, m \tag{18}$$

where K_j is the contribution ratio (%); δ is the assessment values for the F-values; F represents the F-values in the ANOVA table; δ_j is the primary item contribution rate (%); δ_{jj} is the secondary item contribution (%); δ_{ij} is the contribution of the interaction items (%).

3. Results and Discussion

3.1. Effects of Single Factors on Responses

The dimension reduction method was carried out to study the effects of the single factors on the experimental responses. For the model of the percentage of the SCR, the coded independent variables were in turn set at −1.414, −1, 0, 1, and 1.414, whereas the other independent variables were fixed at 0. As shown in Figure 8a$_1$, the *SCR* first increased and then decreased as the coded values of the rotating cracking roller speed (X_2) ascended, and the *SCR* increased with the decreasing cracking angle (X_1), which showed that the appropriate values of X_1 and X_2 could improve the quality of the walnut cracking. The *WKR* increased and then decreased with the increase in X_1 and X_2 in the range of −1.414 to 1.414 (Figure 8b$_1$), which indicated that the *WKR* could be improved with a suitable parameter combination of X_1 and X_2. As shown in Figure 8c$_1$, the *Es* decreased and then increased with the increase in X_1 and X_2 in the range of −1.414 to 1.414, which indicated that the *Es* could be reduced with a suitable parameter combination of X_1 and X_2.

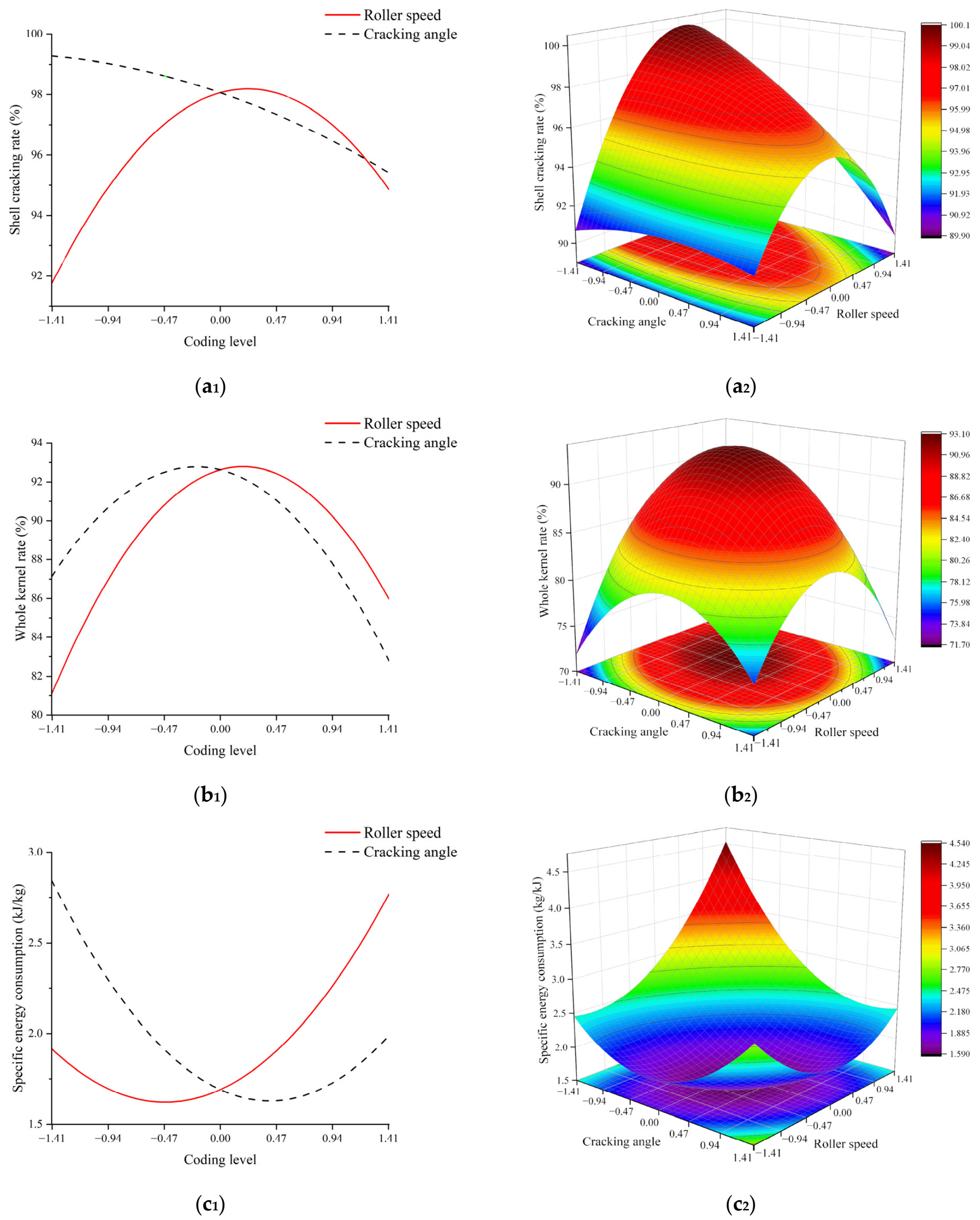

Figure 8. Influence of experimental factors on *SCR* ($\mathbf{a_1}$,$\mathbf{a_2}$), *WKR* ($\mathbf{b_1}$,$\mathbf{b_2}$), *Es* ($\mathbf{c_1}$,$\mathbf{c_2}$).

3.2. Optimization and Verification of Regression Models

3.2.1. Effect of Variables on *SCR*

The measured values of the *SCR* are presented in Table 2. The *SCR* varied between 92.66% and 99.54% with the combinations of the variables studied. According to the ANOVA results shown in Table 3, a second-order polynomial equation was extremely conspicuous ($p < 0.01$) for the responses. There was no significant lack of fit and the high R^2 (0.9232) values showed that most of the variability could be explained by the variables tested. The contributions of each factor affecting the *SCR* were calculated by Equations (17) and (18). The results showed that the RS was the most important factor, followed by the CA. Their contribution ratios were 2.276 and 1.337, respectively. The results in Table 3 indicated that, in this case, the linear term of the CA was extremely significantly different ($p < 0.01$), and the RS was significantly different ($p < 0.05$). The interaction terms of the CA and RS were significantly different ($p < 0.05$). The predicted model for the *SCR* can be described by the following equation in terms of the actual factors under the tested conditions.

$$SCR = 98.06 - 1.36X_1 + 1.10X_2 - 1.15X_1X_2 - 0.36X_1^2 - 2.38X_2^2 \tag{19}$$

Table 3. Analysis of variance (ANOVA) applying response surface quadratic model.

Variation Source	*SCR* Squares	*SCR* df	*SCR* F	*SCR* p	*WKR* Squares	*WKR* df	*WKR* F	*WKR* p	*Es* Squares	*Es* df	*Es* F	*Es* p
β_0	69.3	5	13.86	0.0009 **	275.32	5	26.75	0.0002 **	3.31	5	10.35	0.0039 **
β_1	14.89	1	14.89	0.0038 **	18.81	1	9.14	0.0193 *	0.73	1	11.44	0.0117 *
β_2	9.69	1	9.69	0.0110 *	23.95	1	11.63	0.0113 *	0.73	1	11.39	0.0118 *
$\beta_1\beta_2$	5.24	1	5.24	0.0396 *	14.48	1	7.03	0.0328 *	0.38	1	5.92	0.0453 *
β_{11}	0.9	1	0.9	0.3313	102.01	1	49.55	0.0002 **	0.92	1	14.4	0.0068 **
β_{22}	39.46	1	39.46	0.0002 **	143.98	1	69.94	<0.0001 **	0.74	1	11.58	0.0114 *
R^2		0.9232				0.9503				0.8809		
Lack of fit	4.07	3	1.36	0.1458	6.62	3	1.13	0.436	0.26	3	1.83	0.2823

Note: "**" means extremely significant ($p < 0.01$), "*" means significant ($p < 0.05$).

The representation of the response surface is given in Figure 8a$_2$. The model's expression permits the evaluation of the effects of the factors. As shown in Figure 8a$_1$, the RS was at a level of 0, the CA increased from 0.17° to 0.86°, and the *SCR* dropped from 99.27% to 95.42%. With the increase in the CA, the *SCR* showed a slow decrease. The reason for this behavior was that as the CA increased, the walnuts were subjected to reduced positive pressure and friction between the rotating cracking roller and extrusion plate. When the gap was larger than the size of the walnut, the amount of extrusion deformation decreased, which was not helpful for the expansion of the crack. Some of the walnuts were not completely cracked (lower kernel exposure rate), leading to a decrease in the *SCR*. When the CA was at a level of 0, the *SCR* increased from 91.74% to 98.19% as the RS increased from 63 r/min to 111.89 r/min. The reason was that when the RS was low, the walnuts had enough frictional squeeze to achieve cracking within the gap between the cracking roller and the extrusion plate. When the RS exceeded 111.89 r/min, the *SCR* dropped to 94.86%. There were two possible reasons for this. On the one hand, walnuts were quickly thrown out of the gap between the cracking roller and the extrusion plate, which reduced the friction extrusion enacted upon the walnuts. On the other hand, as the loading speed increased, the amount of shell deformation (walnut shell flexibility) used to break the walnut shells [26] increased, which led to incomplete cracking for a portion of the walnuts. Kilickan and Guner [27] reported that the specific deformation of the olive fruit and pit increased as the compression speed increased. Also, the flexible shell prevented the walnut from cracking [11], which led to a reduced *SCR*.

3.2.2. Effect of Variables on *WKR*

The *WKR* varied from 81.36% to 94.26% with the combinations of the variables (Table 2). The ANOVA results are shown in Table 3 and the model was extremely conspicuous ($p < 0.01$) for the responses. There was no significant lack of fit and the high R^2 (0.9503) values showed that most of the variability could be explained by the variables tested. According to Equations (17) and (18), the factors affecting the *WKR* were the RS (K = 2.329) and the CA (K = 2.299). The results in Table 3 indicate that, in this case, the linear terms of the CA and RS were significantly different ($p < 0.05$). The interaction terms of the CA and RS were significantly different ($p < 0.05$). The predicted model for the *WKR* can be described by the following equation in terms of the actual factors.

$$WKR = 92.62 - 1.53X_1 + 1.73X_2 - 1.90X_1X_2 - 3.83X_1^2 - 4.55X_2^2 \quad (20)$$

The representation of the response surface is given in Figure 8b_2. The model's expression permits the evaluation of the effects of the factors. As shown in Figure 8b_1, when the CA was at a level of 0, the increase in the RS from 63 r/min to 110.53 r/min led to the *WKR* increasing dramatically from 81.08% to 92.78%. Then, the *WKR* declined to 85.97% when the RS increased from 110.53 r/min to 147 r/min. The reason was that the increase in the RS led to a decrease in the fracture force [26], which protected the fragile kernels and increased the *WKR*. When the RS exceeded 105 r/min, the *WKR* dropped sharply. The increase in the specific deformations of the walnut led to damage to the kernel. The kernel had a much smaller fracture force than its shell [28]. Similarly, when the RS was at a level of 0, the CA increased from 0.17° to 0.86° and the *WKR* increased from 87.13% to a maximum of 92.77% (CA = 0.46°) before decreasing to 82.79%. A possible reason for this was that the walnut was subjected to the ideal squeezing pressure for cracking the shell when the gap increased to the thickness of the walnut.

3.2.3. Effect of Variables on *Es*

The values of the *Es* varied from 1.35 kJ/kg to 3.41 kJ/kg as shown in Table 2. Table 3 shows a high correlation coefficient (R^2 = 0.8809) and no significant lack of fit for the responses, indicating that the polynomial fitted well for predicting the *Es*. The CA was the most important factor, followed by the RS, which was obtained by calculating the contribution ratio of the *Es* using Equations (17) and (18). Their contribution ratios were 2.259 and 2.241, respectively. The results in Table 3 indicate that, in this case, the linear terms of the CA and RS were significantly different ($p < 0.05$). The quadratic terms of the CA and RS were significantly different ($p < 0.05$). The predicted model for the *Es* can be described by the following equation in terms of the actual factors.

$$Es = 1.69 - 0.30X_1 + 0.30X_2 - 0.31X_1X_2 + 0.36X_1^2 + 0.33X_2^2 \quad (21)$$

The representation of the response surface is given in Figure 8c_2. The model's expression permits the evaluation of the effects of the factors. As shown in Figure 8c_1, as the CA increased from 0.17° to 0.61°, the *Es* decreased from 2.84 kJ/kg to 1.63 kJ/kg. This is because as the gap between the rotating cracking roller and extrusion plate increased, the walnuts were subjected to less squeezing friction, which lowered the resistance to the roller rotation. As the CA exceeded 0.61°, the *Es* increased with the CA to 1.99 kJ/kg. This was attributed to the fact that the movement of the walnuts in the gap was disordered, which led to increased energy consumption. The *Es* decreased slightly with the increasing RS and then gradually increased. It first decreased from 1.92 kJ/kg to 1.62 kJ/kg and then increased to 2.77 kJ/kg. This was due to the increase in the RS, which increased the power consumption and fracture energy required by the walnuts [29]. The possible reason for the decrease in the *Es* when the RS was less than 90.16 r/min is that at a lower RS, it took longer to complete the cracking of the walnuts. The working time of the cracking device increased, thus the *Es* of the cracking device increased. As the RS increased, the working efficiency also increased, which resulted in a slight decrease in the *Es*.

3.3. Determination and Validation of the Optimal Parameters

In the cracking process, the selection of the CA for the *SCR* and *WKR* was contradictory. Reducing the CA improved the SCR, but when the CA was too small, it reduced the *WKR*. Increasing the CA ensured the quality of the walnut kernels but seriously reduced the *SCR*. To enhance the walnut processing yield, the *WKR* was maximized while retaining a lower *Es* and an appropriate *SCR*. The mathematical models of the *SCR*, *WKR* and *Es* multi-objective functions were constructed, with weights of 0.3, 0.4, and 0.3, respectively. The weights of the *WKR* in the optimization solution equation were set larger than those of the *SCR* and *Es*. Because the magnitudes of the objective functions varied, the linear effectiveness coefficient approach was deployed to turn each objective function into a dimensionless function before applying the respective objective regression equation for comprehensive optimization. The nonlinear programming mathematical model in the following was established by analyzing Equations (19)–(21):

$$\begin{cases} F(X)\begin{cases} Y_1 = \max(SCR) \\ Y_2 = \max(WKR) \\ Y_3 = \min(Es) \end{cases} \\ s.t.\begin{cases} P = \eta_1 Y_1 + \eta_2 Y_2 + \eta_3 Y_3 \\ 0.17^\circ \leq X_1 \leq 0.86^\circ \\ 63\ \mathrm{r/min} \leq \mathrm{X}_2 \leq 147\ \mathrm{r/min} \end{cases} \end{cases} \tag{22}$$

Based on the mathematical model and the regression equations for the *SCR*, *WKR*, and *Es*, the regression equations were optimally solved using MATLAB R2020a (Math-works, Inc. MA, USA) software [30]. The optimum parameters for working were as follows: the CA was 0.47° and the RS was 108.16 r/min. The optimum results were an *SCR* of 98.40%, *WKR* of 92.94%, and *Es* of 1.80 kJ/kg.

The before and after tests of the cracking device optimization are shown in Figure 9 and Table 4. The performance of the walnut cracking using the tip point roller press was superior, and the cracking effect of the walnut cracking device was significantly improved after optimization. Before optimization, the mixture of shells and kernels contained fewer shell-wrapped kernels, relatively intact shells (>1/4 shell), and broken kernels (<1/4 kernel). After optimization, the mixture did not include shell-wrapped kernels but contained many broken shells (<1/8 shell) and relatively intact kernels (>1/4 kernel). Validation experiments were carried out based on the optimal parameters. The measured values of the *SCR*, *WKR*, and *Es* were 97.24%, 92.03%, and 1.88 kJ/kg, respectively, which were close to the predicted values within the acceptable limits of the error percentage (0.98–4.44%). This demonstrates that the regression equations could predict the experimental results from the response surface.

Table 4. Comparison of parameters of cracking device before and after optimization.

Program	CA/(°)	RS/(r/min)	*SCR*/(%)	*WKR*/(%)	*Es*/(kJ/kg)
Before optimization	0.35	150	94.18	56.23	2.12
After optimization	0.47	108	97.24	92.03	1.88

3.4. Variety Adaptability Test

Mixed intercrop planting of multiple species of walnuts is a common phenomenon in Xinjiang, especially in the Hotan and Kashgar regions. Generally, different varieties of walnuts have irregular shapes, large size differences, varying shell thicknesses, and different gaps between the walnut shell and kernel. Previous devices have failed in achieving ideal adaption and cracking performance due to significant differences in the physical properties of the walnut varieties [28,31]. To do this, five common walnut varieties (i.e., 'Wen-185', 'Xinwen-179', 'Xinxin2', 'Zha-343', and 'Xinfeng') were used as test samples to confirm the cracking device's adaptability to the different varieties [23]. In the harvest season of

2021, fresh-harvested walnuts were collected from the Wensu Walnut Experimental Station, Xinjiang, China.

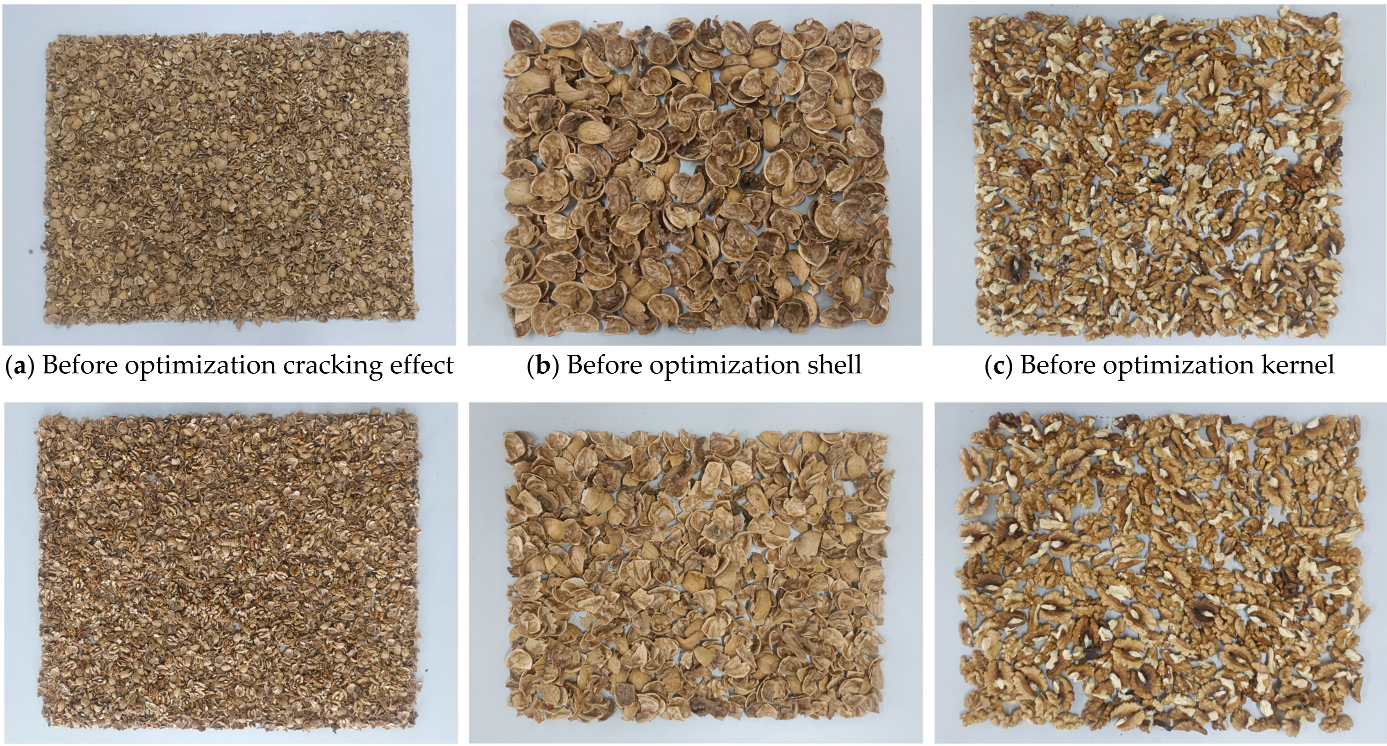

(**a**) Before optimization cracking effect (**b**) Before optimization shell (**c**) Before optimization kernel

(**d**) After optimization cracking effect (**e**) After optimization shell (**f**) After optimization kernel

Figure 9. Prototype experimental conditions, (**a**–**c**) show plots of experimental results before device optimization, and (**d**–**f**) show plots of experimental results after device optimization.

The *t*-test in the IBM SPSS 25.0 (Armonk, NY, USA: IBM Corp) software was used to analyze the significance of the evaluation indicators of the cracking effects of the different varieties of walnuts obtained from the acclimatization trials (Table 5). There were significant differences in the cracking characteristics of the different walnut varieties [5,23]. For the SCR, the cracking unit was well-adapted to the 'Wen-185', 'Xinwen-179', 'Zha-343', and 'Xinxin2' varieties, with an *SCR* greater than 95%. Koyuncu et al. [32] showed that the shell thickness is inversely related to the shell cracking and kernel extraction quality. For the *WKR*, the cracking unit was highly adaptable to the 'Wen-185', 'Xinwen-179', 'Zha-343', and 'Xinfeng' varieties, with a *WKR* greater than 90%. When the walnuts were the same size, the smaller the value of the kernel diameter (t) and the larger the gap between the walnut shell and kernel (d), the greater the deformation allowed by the shell without damaging the kernel, which is conducive to maintaining the integrity of the kernel. For the Es, the cracking unit was highly adaptable to the 'Wen-185', 'Xinwen-179', and 'Zha-343' varieties, with an *Es* of less than 2 kJ/kg. With an increase in the *Es* with increasing shell thickness, similar results were reported by Kacal and Koyuncu et al. (linear relationship) [9,32,33]. In summary, at the same moisture content and size, the cracking device had excellent shelling results for walnuts with a shell thickness (h) < 1.2 mm and a gap between the walnut shell and kernel (d) $\geq$ 1.6 mm.

Table 5. Results of variety adaptability test.

Varieties	Thickness (mm)	Gap between Walnut Shell and Kernel (mm)	*SCR* (%)	*WKR* (%)	*Es* (kJ/kg)
Wen-185	0.86 ± 0.03 a	1.85 ± 0.24 a	97.24 ± 0.41 a	92.03 ± 0.36 a	1.88 ± 0.07 a
Xinwen-179	0.86 ± 0.03 a	1.84 ± 0.24 a	96.54 ± 0.39 a	92.87 ± 0.33 a	1.91 ± 0.08 a
Zha-343	1.16 ± 0.34 a	1.59 ± 0.25 a	96.26 ± 0.54 a	90.07 ± 0.86 a	1.96 ± 0.06 a
Xinxin-2	1.20 ± 0.11 a	1.57 ± 0.11 b	95.99 ± 0.42 a	84.83 ± 1.29 b	2.41 ± 0.12 b
Xinfeng	1.48 ± 0.15 b	1.67 ± 0.26 a	84.62 ± 0.40 b	92.11 ± 0.39 a	3.24 ± 0.11 b

Note: Data in the table are "mean ± standard deviation" of samples, different letters in the same column indicate significant differences ($p < 0.05$).

Wang et al. [17] conducted walnut cracking experiments and discovered that walnut moisture content had a significant impact on the cracking quality. Zheng et al. [23] reported that the shell thickness and geometric mean diameter affected the quality of kernel extraction from cracked walnuts. In this paper, we also found a significant effect of the gap between the walnut shell and kernel on the cracking effect of walnuts. There was a relationship between the shell thickness and the energy consumption of the cracking quality, which is shown in Table 5. Therefore, the material properties (shell thickness, moisture content, gap between walnut shell and kernel, etc.), walnut cracking characteristics (cracking force, cracking energy, power of walnut cracking, etc.) and the correlation between them for the different walnut varieties still need to be studied in depth.

4. Discussion

The different types of walnut cracking devices were compared and the results are listed in Table 6 [9,10,12,17,34–36]. It is clear that compared to other types, the extrusion type had a higher working efficiency [22,36]. In addition, the load with multiple contact points was significantly better than a pair of forces and two pairs of forces, showing a larger *SCR* and *WKR*. Studies have suggested that single point or line loads cause uneven forces on the shell, poor crack extension, and damage to the kernels [13]. However, multi-point walnut cracking not only contributes to crack generation and expansion but also reduces the stress value and deformation used to break walnut shells on the condition that the kernel stays whole [8]. Additionally, it is worth pointing out that many walnut cracking devices only focused on the improvement of the *SCR* but ignored the *WKR*. Fortunately, the walnut cracking device designed in this work considered simultaneously a larger *SCR* and *WKR*. Nonetheless, the following two points of the multi-point extrusion type walnut cracking device need to be further enhanced.

(1) The multi-point extrusion walnut cracking device is integrated with walnut grading and walnut cracking, where the accuracy of the grading affects the cracking performance. The mixed grade of the walnuts causes a mismatch between the size of the walnuts and the cracking angle, which indirectly affects the cracking performance of the walnut cracking device [36]. The accuracy of grading needs to be further improved.

(2) The posture of the walnut falling into the gap between the rotating cracking roller and extrusion plate after grading is generally random. Therefore, it is necessary to seek a directional cracking device that can realize the breakage of the walnut shell, which is beneficial for improving walnut cracking.

Table 6. Comparison of different types of walnut cracking devices.

Principle	Name	Loading Style	Results of Cracking
Shear type	Walnut shearing extrusion flexible shell-crushing device [9]	Two pairs of forces	*WKR* = 75%, *SCR* = 98%
	6HP-400 cone basket walnut shelling device [34]	Two pairs of forces	*WKR* = 90.3%, *SCR* = 97.3%
Impact type	Conic roller shelling device based on walnut moisture-regulating treatments [17]	A pair of forces	*WKR* = 84.54%, *SCR* = 99.15%
	Secondary shell-breaking machine for pecans [35]	A pair of forces	*WKR* = 83.86%, *SCR* = 87.58%, Ph = 500 kg/h
Extrusion type	Clearance walnut sheller [10]	A pair of forces	*WKR* = 83.6%, *SCR* = 94%
	Cam rocker bidirectional extrusion walnut shell-breaking device [12]	Two pairs of forces	*WKR* = 61.39%, *SCR* = 92.36%
	Squeezed walnut shell-breaking machine with self-grading and multi-station [36]	Two pairs of forces	*WKR* = 84.72%, *SCR* = 91.5%
	Multi-point extrusion walnut cracking device	Multiple pairs of forces	*WKR* = 92.03%, *SCR* = 97.24%, *Es* = 1.88 kJ/kg, Ph = 850 kg/h

Note: Ph walnut cracking efficiency.

5. Conclusions

The present work described an engineering solution to the walnut cracking problem. A machine for cracking walnuts was designed and manufactured and also evaluated for performance. The response surface test results showed that all the parameters had a significant influence on the three indicators, whereas only the CA had an extremely significant effect on the *SCR*. The obtained regression equation could be used to quantitatively predict the cracking quality under different operating parameters. Taking all the indices into comprehensive consideration, the machine performance was found to be optimum at a CA of 0.47° and an RS of 108 r/min. For the 'Wen-185' walnut, the *SCR*, *WKR*, and *Es* were 97.24% against the predicted 98.40%, 92.03% against the predicted 92.94%, and 1.88 kJ/kg against the predicted 1.80 kJ/kg, respectively. The variety adaptability tests showed that the cracking device was well-adapted to the 'Wen185', 'Xinwen-179', and 'Zha-343' varieties. The cracking device had excellent cracking results for walnuts with a shell thickness (h) < 1.2 mm and a gap between the walnut shell and kernel (d) $\geq$ 1.6 mm, for example, the 'Wen-185', 'Xinwen-179', 'Zha-343' varieties, as well as other walnut varieties with thin shells and a larger gap between the walnut shell and kernel. This paper provides a theoretical reference for improving and optimizing walnut cracking devices' processing parameters.

Author Contributions: Conceptualization, H.Z. and Y.Z.; methodology, H.L.; software, H.L.; validation, Y.T.; formal analysis, J.C.; investigation, H.L.; resources, H.Z.; data curation, H.L.; writing—original draft preparation, H.L.; writing—review and editing, H.Z. and Y.Z.; visualization, H.L. and Z.Z.; supervision, H.Z. and Y.Z.; project administration, Y.T.; funding acquisition, H.Z. All authors have read and agreed to the published version of the manuscript.

Funding: This research was financially supported by the Chinese Natural Science Foundation (12002229, 31160196), the President's Foundation of Tarim University (TDZKBS202001), the Open Project of the Modern Agricultural Engineering Key Laboratory (TDNG2022101, TDNG2021104), and the Shishi Science and Technology Program (Grant No. 2021ZB01).

Institutional Review Board Statement: Not applicable.

Informed Consent Statement: Not applicable.

Data Availability Statement: The data presented in this study are available on request from the corresponding author.

Acknowledgments: The authors express their thanks to the Chinese Natural Science Foundation (12002229, 31160196), the President's Foundation of Tarim University (TDZKBS202001), the Open Project of the Modern Agricultural Engineering Key Laboratory (TDNG2022101, TDNG2021104), and the Shishi Science and Technology Program (Grant No. 2021ZB01) for their financial support and to all of the people who assisted with the writing of this paper. The authors are grateful to the anonymous reviewers for their comments.

Conflicts of Interest: The authors declare no conflict of interest.

Abbreviations

CA	Cracking Angle
RS	Roller Speed
SCR	Shell-Cracking Rate
WKR	Whole Kernel Rate
Es	Specific Energy Consumption
CCD	Central Composite Design
RSM	Response Surface Methodology
ANOVA	Analysis of Variance

References

1. Ghafari, A.; Chegini, G.R.; Khazaei, J.; Vahdati, K. Design, construction and performance evaluation of the walnut cracking machine. *Int. J. Nuts Relat. Sci.* **2011**, *1*, 70–74.
2. Geng, S.; Ning, L.; Ma, T.; Chen, H.; Zhang, Y.; Sun, X. Comprehensive analysis of the components of walnut kernel (*Juglans regia* L.) in China. *J. Food Qual.* **2021**, *95*, 825–834. [CrossRef]
3. Sütyemez, M.; Bükücü, Ş.B.; Özcan, A. 'Helete Güneşi', a New Walnut Cultivar with Late Leafing, Early Harvest Date, and Superior Nut Traits. *Agriculture* **2021**, *11*, 991. [CrossRef]
4. Brunner-Parra, C.F.; Croquevielle-Rendic, L.A.; Monardes-Concha, C.A.; Urra-Calfuñir, B.A.; Avanzini, E.L.; Correa-Vial, T. Web-Based Integer Programming Decision Support System for Walnut Processing Planning: The MeliFen Case. *Agriculture* **2022**, *12*, 430. [CrossRef]
5. Bernik, R.; Stajnko, D.; Demsar, I. Comparison of the kernel quality of different walnuts (*Juglans regia* L.) varieties shelled with modified centrifugal sheller. *Erwerbs-Obstbau* **2020**, *62*, 213–220. [CrossRef]
6. Liu, M.; Li, C.; Zhang, Y.; Wang, L. Advances and recent patents about cracking walnut and fetching kernel device. *Recent Pat. Mech. Eng.* **2015**, *8*, 44–58. [CrossRef]
7. Wang, W.; Wang, Y.; Wang, P.; Lu, J.; Tian, Z. Structure improvement design and test of cone basket walnut shelling. *J. Agric. Mech. Res.* **2022**, *44*, 124–129.
8. Ding, R.; Cao, C.; Zhan, C.; Lou, S.; Sun, S. Design and experiment of bionic-impact type pecan shell breaker. *Trans. Chin. Soc. Agric. Eng. Trans. CSAE* **2017**, *33*, 257–264.
9. Liu, M.; Li, C.; Zhang, Y.; Yang, M.; Hou, Y.; Gao, L. Shell crushing mechanism analysis and performance test of flexible-belt shearing extrusion for walnut. *Trans. Chin. Soc. Agric. Mach.* **2016**, *47*, 266–273.
10. Li, X. *Parameters Optimization of Clearance Walnut Sheller*; Sichuan Agricultural University: Ya'an, China, 2018.
11. Sharifian, F.; Derafshi, M.H. Mechanical behavior of walnut under cracking conditions. *J. Appl. Sci.* **2008**, *8*, 886–890. [CrossRef]
12. Shi, M.; Liu, M.; Li, C.; Cao, C.; Li, X. Design and Experiment of Cam Rocker Bidirectional Extrusion Walnut Shell Breaking Device. *Trans. Chin. Soc. Agric. Mach.* **2022**, *53*, 140–150.
13. Cao, C.; Jiang, L.; Wu, C.; Li, Z.; Wang, T.; Ding, R. Design and test on hammerhead of pecan shell-breaking machine. *Trans. Chin. Soc. Agric. Mach.* **2017**, *48*, 307–315.
14. Zhang, H.; Shen, L.; Lan, H.; Li, Y.; Liu, Y.; Tang, Y.; Li, W. Mechanical properties and finite element analysis of walnut under different cracking parts. *Trans. Chin. Soc. Agric. Eng. Trans. CSAE* **2018**, *11*, 81–88. [CrossRef]
15. Shen, L. *Design and Experimental Study on the Walnut Cracking Machine with Impact Extrusion Type*; Tarim University: Alar, China, 2017.
16. He, Y.; Wang, X.; Cao, S.; Wang, M.; Liu, H. Design and experimental study of a roller extrusion type walnut shell breaking device. *Jiangsu Agric. Sci.* **2012**, *40*, 350–352.
17. Wang, J.; Liu, M.; Wu, H.; Peng, J.; Peng, B.; Yang, Y.; Cao, M.; Wei, H.; Xie, H. Design and key parameter optimization of conic roller shelling device based on walnut moisture-regulating treatments. *Agriculture* **2022**, *12*, 561. [CrossRef]
18. Man, X. *Optimization of the Process Parameters of Hot-Air and Microwave-Vacuum Synergistic Drying for Walnut Shell Breaking*; Tarim University: Alar, China, 2021.
19. Zeng, Y.; Jia, F.; Meng, X.; Han, Y.; Xiao, Y. The effects of friction characteristic of particle on milling process in a horizontal rice mill. *Adv. Powder Technol.* **2018**, *29*, 1280–1291. [CrossRef]
20. Ashok, G.; Denis, Y. Chapter 6—Roll Crushers, Mineral Processing Design and Operation; Elsevier Science: 2016. Available online: https://www.elsevier.com/books/mineral-processing-design-and-operations/gupta/978-0-444-63589-1 (accessed on 8 August 2022).
21. Hu, Y.; Li, J.; Lu, H.; Xiao, H. Design and experiment of equant-diameter roller screening machine for fresh tea leaves. *Trans. Chin. Soc. Agric. Mach.* **2015**, *46*, 116–121.

22. Liu, M.; Li, C.; Cao, C.; Wang, L.; Li, X.; Che, J.; Yang, H.; Zhang, X.; Zhao, H.; He, G.; et al. Walnut fruit processing equipment: Academic insights and perspectives. *Food Eng. Rev.* **2021**, *13*, 822–857. [CrossRef]
23. Zheng, X.; Zhang, E.; Kan, Z.; Zhang, H.; Li, H.; Chou, W. Improving cracking characteristics and kernel percentage of walnut by optimal position of cutting on shell. *Trans. Chin. Soc. Agric. Eng. Trans. CSAE* **2018**, *34*, 300–308.
24. Meng, X.; Jia, F.; Xiao, Y.; Han, Y.; Zeng, Y.; Li, A. Effect of operating parameters on milling quality and energy consumption of brown rice. *J. Food Sci. Technol.* **2019**, *56*, 674–682. [CrossRef]
25. Shen, G.; Wang, G.; Hu, L.; Yuan, J.; Wang, Y.; Wu, T.; Chen, X. Development of harvesting mechanism for stem tips of sweet potatoes. *Trans. Chin. Soc. Agric. Eng. Trans. CSAE* **2019**, *35*, 46–55.
26. Altuntas, E.; Erkol, M. The effects of moisture content, compression speeds, and axes on mechanical properties of walnut cultivars. *Food Bioprocess Technol.* **2011**, *4*, 1288–1295. [CrossRef]
27. Kilickan, A.; Guner, M. Physical properties and mechanical behavior of olive fruits (*Olea europaea* L.) under compression loading. *J. Food Eng.* **2008**, *87*, 222–228. [CrossRef]
28. Gharibzahedi, S.M.T.; Mousavi, S.M.; Hamedi, M. Mechanical behavior of Persian walnut and its kernel under compression loading: An experimental and computational study. *J. Food Process. Preserv.* **2008**, *36*, 423–430. [CrossRef]
29. Khazaei, J.; Rasekh, M.; Borghei, A.M. *Physical and Mechanical Properties of Almond and Its Kernel Related to Cracking and Peeling*; Cambridge Universuty Press: Chicago, IL, USA, 2002.
30. Yang, R.; Chen, D.; Zha, X.; Pan, Z.; Shang, S. Optimization design and experiment of ear-picking and threshing devices of corn plot kernel harvester. *Agriculture* **2021**, *11*, 904. [CrossRef]
31. Ebubekir, A.; Yakup, O. Physical and mechanical properties of some walnut (*Juglans regia* L.) cultivars. *Int. J. Food Eng.* **2008**, *4*, 99–107.
32. Koyuncu, M.A.; Ekinci, K.; Gun, A. The effects of altitude on fruit quality and compression load for cracking of walnuts (*Juglans regia* L.). *J. Food Qual.* **2004**, *27*, 407–417. [CrossRef]
33. Kacal, M.; Koyuncu, M.A. Cracking characteristics and kernel extraction quality of hazelnuts: Effects of compression speed and positions. *Int. J. Food Prop.* **2017**, *20*, 233–240. [CrossRef]
34. Wang, W.; Tian, Z.; Wang, P.; Wang, Y. Design and experiment of 6HP-400 cone basket walnut shelling. *Packag. Food Mach.* **2021**, *39*, 84–88.
35. Cao, C.; Li, Z.; Luo, K.; Wang, T.; Wu, Z.; Xie, C. Design and experiment of secondary shell breaking machine for Pecan. *Trans. Chin. Soc. Agric. Mach.* **2019**, *50*, 128–135.
36. Liu, X. *Development and Test of a Squeezed Walnut Shell Breaking Machine with the Self-Grading and Multi-Station*; Southwest University: Chongqing, China, 2021.